IEEE Access
Multidisciplinary ⋮ Rapid Review ⋮ Open Access Journal

Received March 16, 2022, accepted April 17, 2022, date of publication April 21, 2022, date of current version April 29, 2022.

Digital Object Identifier 10.1109/ACCESS.2022.3169443

Assessing Repeatable Accuracy Potential of LoRa: A Navigation Approach

CASPAR K. LEBEKWE, (Member, IEEE), LONE KOLOBE, BOYCE SIGWENI, (Member, IEEE), AND ADAMU MURTALA ZUNGERU, (Senior Member, IEEE)

Department of Electrical, Computer and Telecommunications Engineering, Botswana International University of Science and Technology, Palapye, Botswana

Corresponding authors: Caspar K. Lebekwe (lebekwec@biust.ac.bw) and Adamu Murtala Zungeru (zungerum@biust.ac.bw)

This work was supported in part by the Department of Electrical, Computer and Telecommunications Engineering, Botswana International University of Science and Technology (BIUST).

ABSTRACT Two main classes of radio navigation systems are satellite and ground-based systems. Examples of such systems are eLoran deployed as a terrestrial system, and BeiDou, Galileo, GPS and Quasi-Zenith Satellite System (QZSS) deployed as satellite Navigation Systems. These systems have been investigated in different navigation use-cases using a hybrid receiver capable of receiving any navigation signal. The goal of this paper is to demonstrate LoRa's capability as a signal of opportunity (SoOP) to be used with other navigation technologies in order to improve repeatable accuracy. While researchers have investigated LoRa's potential for navigation purposes, there is limited literature regarding the repeatable accuracy estimation using LoRa. Our work proposes using a weighted horizontal dilution of precision (HDOP) while incorporating SNR, spreading factors (SF) and the Ericsson 9999 path loss model. The gateway separation distances: 1500 m, 1000 m and 400 m respectively are employed at a bandwidth of 125kHz to determine repeatable accuracy within a 95% confidence limit. Our simulation results show that for 1500 m, 1000 m, and 400 m, gateway separation distances have a best repeatable accuracy of 1249 m, 284.2 m and 4.314 m, respectively, when the spreading factor (SF) is equal to 12. The initial repeatable accuracy results are promising and comparable to those obtained by other researchers. Our model's limitation is that the best SNR was not used to determine position. A climatic model and stochastic channel interference observed in the 900MHz frequency band were also assumed to be negligible to provide a working model that can be modified as data becomes available.

INDEX TERMS LoRa navigation, eLoran, LPWAN navigation, signals of opportunity.

I. INTRODUCTION

Navigation is key in modern recreation sectors such as drone flying, in commercial agriculture for geo-fencing animals and smart harvesters or in military/combat scenarios [1], [2]. Specifically, it uses radio signals to determine the target's location. The main classes of radio navigation systems are satellite and ground-based navigation systems. For both of these systems, repeatable accuracy is the conformance of the current position to the previously measured position obtained using the same navigation system [3]. This system performance parameter may prove useful in LoRa use-cases to locate maintenance hole covers hidden by vegetation in unpopulated areas of Africa. Other systems such as are eLoran, Omega and DECCA and BeiDou, Galileo, GPS, and Quasi-Zenith Satellite System (QZSS) have been deployed in the past for navigation purposes [4] as stand-alone systems. The stand-alone usage of terrestrial technologies resulted in coverage gaps as the user moved from one location to another due to signal loss and interference. Over time as the need for navigation solutions increased, it became critical to fill in the coverage gaps within a specified area by integrating signals from several technologies. Researchers have put more effort into building state of the art receivers with a capability to navigate using a combination of radio signals from these navigation technologies. This receiver signal processing hybridisation has resulted in the investigation of pseudorange errors obtained using the signals of opportunity (SoOP) [5]. Platforms that take advantage of SoOP incorporate low power alternatives such as LoRa to provide novel opportunities to network designers/engineers in the Internet of things (IoT) and Intenet of Lives (IOL) landscapes. SoOp is important

The associate editor coordinating the review of this manuscript and approving it for publication was Tianhua Xu.

where high degrees of accuracy is sought after at a fraction of the cost of deployment of traditional navigation systems.

Different navigation scenarios use technologies that best suit required system performance parameters such as accuracy, availability, continuity and integrity [6]. In the case of civil aviation, an aircraft will often operate in a developed region with a ground-based radio navigation system to assist in take-off and landing phases. A satellite-based system is ideal for flight scenarios such as moving over the ocean or undeveloped regions [4]. Accuracy is vital in an eLoran Harbour Entrance and Approach (HEA) manoeuvres use case. Performance requirements for each system parameter vary from one use case to another and are documented by several regulatory bodies such as International Maritime Organisation (IMO), which deals specifically with maritime affairs and standards [7].

There is a growing interest to employ LoRa for ranging or localisation when using low power vast area network (LPWAN) technology. The advantage is that LoRa has a long battery life documented to be two years when using two AA batteries. The deployed battery-powered nodes transmit packets using the LoRaWAN protocol and chirp spread spectrum modulation (CSS) [8]. Additionally, LoRa has reported ranges of several kilometres, with some deployments showing a range of hundreds of kilometres when using 25 mW of transmission power. Mini satellites deployments and weather balloons have exploited this range capability [9].

We present a LoRa repeatable accuracy model that may be useful when LoRa is used as a signal of opportunity in applications such as eLoran Harbour Entrance and Approaches, where accuracy is critical. LoRa's long battery power and long-range capability make it suitable for such applications.

A. CONTRIBUTIONS

Our research shows that most of the frequently cited work in LoRa localisation or navigation focuses on either the TDOA method or the RSSI method of localisation. In summary, the contributions of this research are as follows:

- The CRLB derived variance of the TOA of a LoRa packet combined with weighted HDOP to determine position accuracy.
- Demonstrate the capability of LoRa's repeatable accuracy in the coverage area at 1500 m, 1000 m and 400 m separation distances for spreading factors equal to 7, 8, 10, and 12.

The organisation of the rest of this article is as follows: section III presents a background into the theory underlying our work. Section IV-A details our experimental setup, section V provides the simulation results and analysis of our findings, while the last section VI concludes the work as well as proposes future work in LoRa localisation.

II. RELATED WORKS

The literature presents repeatable accuracy for several navigation systems. Johnson *et al.* [5] exploited several radio navigation system signals to demonstrate the capability and improved accuracy performance of a proposed receiver architecture that can process such signals. Although LoRa was not part of the system whose signals the proposed receiver design could process, this work highlights LoRa as a valuable and potential candidate to that list. Table 1 summarises the most cited work in the growing research area of LoRa navigation.

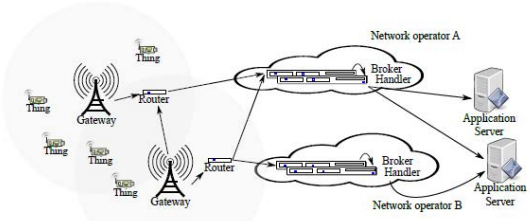

FIGURE 1. LoRa LPWAN architecture [15].

III. BACKGROUND

This section introduces LoRa localisation methods, precisely the Time of arrival (TOA) variance method. The LoRa signal's TOA variance is dependent on its strength determined from known path-loss models, spreading factor, bandwidth, signal to noise ratio and the sampling period. Lastly, it discusses several LoRa accuracy techniques.

A. LOCALISATION IN LoRa

Figure 1 shows a typical LPWAN architecture where the end nodes transmit packets via a wireless channel to a gateway. Generally, gateways are hybrid transceivers with access to WIFI, GSM or a satellite link to transmit end node data to the cloud, using an appropriate protocol, such as Message Queue Telemetry Transport (MQTT) for delivery to an application server. The end nodes may be stationary or mobile while fixing gateways at known locations.

The standard position accuracy determination method for LoRa uses time difference of arrival (TDOA) variance. In this method, an end node (LoRa transceiver) will transmit a timestamped packet, which will need to be received by at least three gateways; otherwise, the node's position cannot be determined [12], [14]. The packet timestamp is at the node, gateway and application server. The difference between the packet's transmission timestamp by the node and the time stamp at the gateway upon reception is the propagation time. The Signal to Noise (SNR), coding rate (CR), RSS and frequency deviation due to Doppler shift is determined or retrieved at the gateway. These parameters are then sent to the application server for the position accuracy determination [10], [13]. However, TDOA range estimations are limited by two significant factors, namely multipath propagation and clock accuracies [12], [14]. Alternatively, a received signal strength indicator (RSSI) may be used but is not discussed in this paper. Another localisation method that takes into account the SNR, spreading factor (SF) and bandwidth (BW) is the TOA variance and is derived using maximum likelihood principles, specifically the Cramer Rao Lower Bound

TABLE 1. LoRa navigation or geolocation articles.

Source	Summary	Year	Citations
[10]	The authors of this article proposed three objectives: to quantify the performance of a TDOA based navigation algorithm on a public LoRa network in the Netherlands for three movement types; walking, cycling and driving. Secondly, they determined the best LoRa spreading factor concerning updating absolute position accuracy frequently. Third, the researchers assess the improvements when using a tracking algorithm that considers the roadmap and the movement speed of the user. The experiment showed a 90^{th} percentile repeatable accuracy of 579 m, 490 m,324 m for walking, cycling and driving, respectively, with transmission ranges of 10 km -34 km. Lastly, their experiment revealed that the SF that balances range, frequency of position updates and energy consumption was SF 8. Due to the use of a public network, the authors were unable to properly account for the influence of HDOP on the ranging errors. Lastly, their work focuses on the TDOA method and absolute accuracy rather than repeatable accuracy.	2018	37
[11]	The researchers of this work investigated the viability of ranging algorithms for LoRa based on TOA, TDOA, RSSI and a phased based approach (proposed by the researchers). This work determines through a combination of, presentation of observations from other authors and mathematical analysis that phase-based localisation may be the best to improve LoRa repeatable accuracy. Specifically getting it to GPS and WiFi repeatable accuracies of under 5 m. The authors cite significant signal attenuation following barrier penetration, a smooth time domain signal waveform, and low-resolution internal clocks as limitations for TDOA, TOA, and RSSI.	2018	7
[12]	This whitepaper by LoRa details the potential viability of LoRa for navigation. The document highlights key concepts such as the influence of transmitter-receiver geometry on position errors. Additionally, the authors summarise the TDOA method of localisation and give documented application scenarios from animal tracking to waste tracking.	2018	3
[13]	The authors of this work proposed two TDOA based algorithms to estimate the position of a stationary point. Their experiment in Denmark used four gateways encompassing an area of approximately $9km^2$. Using their algorithm, they achieved a repeatable accuracy of 100 m. However, the authors did not provide details of the specific SF, BW, or CR used. Lastly, their work focusses specifically on the TDOA method	2017	100

(CRLB) [14]. For LoRa, the CRLB can be used to determine TOA variance of a single packet received at the gateway [14], [16] and is given by:

$$CRLB = \frac{1}{E[\frac{\delta}{\delta\psi}\ln p(N|\psi)]} \tag{1}$$

$$CRLB = \frac{1}{-E[\frac{\delta}{\delta\psi}\ln p(N|\psi)]} \tag{2}$$

[14] where:

- E is the expectation or statistical average,
- N is the influence of various features including multipath, SNR etc,
- ψ is the desired entity.

The received signal $y[n]$, is discretized by sampling at Nyquist $T_s = \frac{1}{k2BW}$, where k is the oversampling ratio.

$$y[n] = \sum_{n=0}^{M-1} a_m s[n] + w[n] \tag{3}$$

where $s[n]$ is the transmitted packet, a_m is the amplitude of the transmitted signal and $w[n]$ is the noise.

Assuming the variance of $y[n]$ is given by σ^2, the noise $w[n]$ has an average and variance of N_0B, N_0 respectively. When sampling at Nyquist, the received samples may be assumed to be uncorrelated and contaminated with Gaussian noise.

$$p(y[n]) = \frac{1}{\sqrt{(2\pi\sigma^2)}}\exp^{\frac{1}{2\sigma^2}[y[n]-s[n]]^2} \tag{4}$$

$$p(y;\tau) = \frac{1}{(2\pi\sigma^2)^{(\frac{N}{2})}}\exp^{\frac{-1}{2\sigma^2}\sum_{n=0}^{N-1}[y[n_i]-s[n_i\tau]]^2} \tag{5}$$

The denominator in equation 2 is known as the Fisher information matrix and can be in a form shown in 6. In this mode, the assumption is that the range information is dependent on the TOA of the received signal [16]. $E[\frac{\delta^2}{\delta\psi}\ln p(y|\tau)]$ can therefore be used to determine the CRLB of TOA variance.

$$E[\frac{\delta^2}{\delta\psi}\ln p(y|\tau)] = \frac{1}{\sigma^2}\sum_{n=0}^{N-1}(y[n]-s[n])\frac{\delta^2 s[n]}{\delta\tau^2} - (\frac{\delta s[n]^2}{\delta\tau})^2 \tag{6}$$

$$var(\tau) \geq E[\frac{\delta^2}{\delta\psi}\ln p(y|\tau)] \tag{7}$$

$$var(\tau) = \frac{\sigma^2}{\sum_{n=0}^{N-1}(\frac{\delta s[n]}{\delta\tau})^2} \tag{8}$$

If the sampling period is assumed to be small, then the denominator in equation 8 may be approximated using an integration operation from $t = 0 - T_s$.

$$var(\tau) \geq CRLB \geq \frac{\sigma^2}{\frac{1}{T_s}\int_0^{T_s}(\frac{ds(t)}{dt})^2 dt} \tag{9}$$

According to [14], the CRLB may be expressed as:

$$CRLB = \frac{1}{\frac{\epsilon}{\frac{N_0}{2}}\bar{F^2}} \tag{10}$$

where $\bar{F^2}$ is given by

$$\bar{F^2} = \frac{\int_{-\infty}^{\infty}(s\pi F)^2|S(F)|^2dF}{\int_{-\infty}^{\infty}|S(F)|^2dF} \tag{11}$$

Ming et. al [16] showed that

$$\epsilon = \int_0^{T_s}|s(t)|^2dt = T_{sym}\int_{-\infty}|S(F)|^2. \tag{12}$$

Simplifying equation 12 leads to

$$\epsilon = T_{sym}BW|S(F)|^2 \tag{13}$$

Simplifying equation 11 leads to:

$$\bar{F^2} = \frac{4\pi^2(BW)^2}{3} \tag{14}$$

The TOA variance of a received LoRa CSS signal with a known SNR is showed by equation 15.

$$var(D) = \frac{3c}{8\pi^2KT_{sym}(BW)^3SNR} \tag{15}$$

Each modulation SF requires a minimum SNR value necessary for successful signal detection [17]. This SNR threshold results in a maximum TOA variance threshold. Table 2 shows maximum TOA values for different SFs at their SNR threshold. The minimum SNR values determine the sensitivity of deployment using 17. Figure 2 and 3 illustrate the pseudo-range error performance for SNR versus SF and SNR versus bandwidth, respectively. It is important to note that the complete TOA algorithm must include all factors contributing to the signal's arrival time variance. The following form expresses the TOA variance using the error propagation laws:

$$\sigma^2_{TOA} = \sigma^2_{SNR} + \sigma^2_{Weather} + \ldots + \sigma^2_{unknown} \tag{16}$$

where σ^2_{SNR} is the variance in TOA due to SF, SNR, bandwidth, while $\sigma^2_{Weather}$ is the TOA variance due to weather changes along the propagation path between the end node and the gateway. In this study, we assume that the $\sigma^2_{Weather}$ is negligible, and $\sigma^2_{unknown}$ represents the TOA variance due to other unknown error sources. According to [18], receiver sensitivity is given by:

$$S_{min} = -174 + 10\log(BW) + NF + SNR_{Limit} \tag{17}$$

where:

- S_{min} is the minimum receiver sensitivity,
- BW represents the modulation bandwidth,
- NF is the noise floor and is fixed at $6dB$ for SX1272 and SX1276 transceiver chips,
- SNR_{Limit} is the minimum detectable SNR for a given spreading factor

TABLE 2. Pseudorange error performance at minimum SNRs using various SFs.

Modulation (SF)	SNR (dB)	Pseudorange error(m)
7	-7.5	98
8	-10.0	92
9	-12.5	87
10	-15.0	82
11	-17.5	78
12	-20.0	73

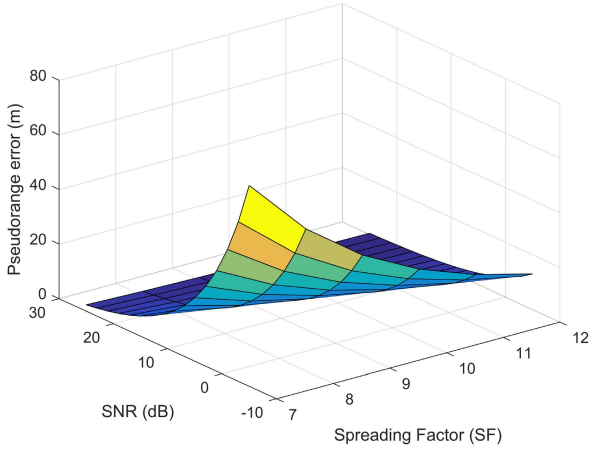

FIGURE 2. Pseudorange error performance with respect to SNR and the spreading factors.

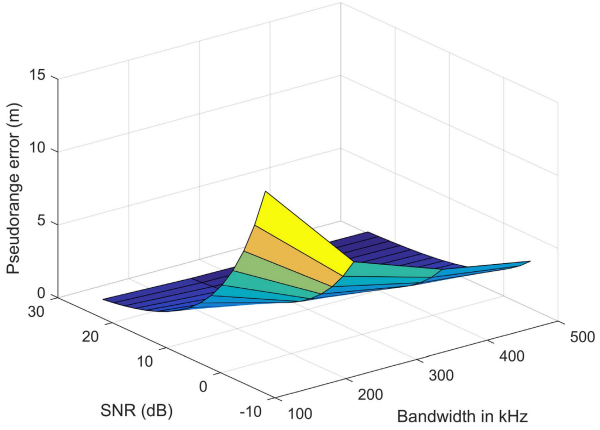

FIGURE 3. Pseudorange error performance with respect to SNR and Bandwidths.

B. GEOMETRY AND SIGNAL STRENGTH OF LoRa GATEWAYS

The distances between gateways and the bearings of receivers to gateways, signal strength, and SNR influences position accuracy. The horizontal dilution of precision (HDOP) includes the effects of the receiver bearing from the transmitters. The design matrix and the signal SNRs form a weighted HDOP. The pseudo-range error evaluation is described in [5], [19]. The maximum likelihood, specifically CRLB, is used to describe The TOA variance of a LoRa signal. The TOA variance is given by:

$$\sigma^2_D(m) = \frac{3c^2F_s}{8\pi^2kB^3SNR} \tag{18}$$

Equation 18 represents the TOA variance in square meters. where:

- c is light propagation speed $299792458m/s$,
- B LoRa specified bandwidth and may be stated as 125kHz, 250kHz and 500kHz,
- SNR is signal to noise ratio,
- σ_τ^2 is the TOA variance,
- SF represents the LoRa signal's spreading factor.
- k is the time index, normally set to 1 to make sampling frequency to be equal to the Nyquist frequency,
- F_x represents the sampling frequency.

The number of received samples is determined by:

$$N_s = F_x \times \frac{2^{SF}}{B} \tag{19}$$

The following form represents the time of arrival variance in square meters at the Nyquist frequency:

$$\sigma_\tau^2(m) = \frac{G_{Lora}}{N_s \times SNR} \tag{20}$$

where G_{Lora} is given by $\frac{3c^2 2^{SF}}{8\pi^2 kB^4}$. The TOA variances are the entries of the covariance matrix described in [3], [19]. The resulting covariance matrix is:

$$\sigma^2(\tau) = \begin{Bmatrix} \sigma_{11}^2 & \sigma_{21} & \sigma_{31} \\ \sigma_{12} & \sigma_{22}^2 & \sigma_{32} \\ \sigma_{31} & \sigma_{32} & \sigma_{33}^2 \end{Bmatrix} \tag{21}$$

[20]

The assumed mutually uncorrelated and Gaussian distributed pseudorange measurement error is determined by the square root of equation 20. Under this assumption, the off-diagonal elements in the covariance matrix shown by equation 21 are set to zero. The entries of the covariance matrix are formed using The TOA variances of the received signals. The inverse of the covariance is used as a weighting in the receiver's position calculation. This ensures that gateways with better SNR contribute more to the position solution. [3], [19].

$$\sigma^2(\mu) = \begin{Bmatrix} \sigma_{11}^2 & 0 & 0 \\ 0 & \sigma_{22}^2 & 0 \\ 0 & 0 & \sigma_{33}^2 \end{Bmatrix} \tag{22}$$

The least squares approach is used to determine repeatable accuracy at the LoRa receiver's location [20]. As shown in equation 24 square root of the trace of equation 21 is equal to the HDOP. where G is the design matrix [19]. Equation 23 shows the design matrix.

$$G = \begin{Bmatrix} sin(\eta_1) & cos(\eta_1) & 1 \\ sin(\eta_2) & cos(\eta_2) & 1 \\ sin(\eta_3) & cos(\eta_3) & 1 \\ sin(\eta_n) & cos(\eta_n) & 1 \end{Bmatrix} \tag{23}$$

where α_n represents the bearings of the gateways (Tx) from the receiver (Rx) nodes. The weighted HDOP is given by:

$$HDOP = \sqrt{tr(G^T WG)^{-1}} \tag{24}$$

where G represents the weight matrix equivalent to σ_D^2. HDOP in a coverage area is determined as follows:

- Geographical area is divided into equally spaced grid points
- A minimum of three gateways located in the coverage area are used
- Design matrix is determined at each grid point formed from sines and cosine of the gateway bearings from the mobile node
- The TOA variance of each gateway signal at every grid point is calculated
- The weighted HDOP is determined

This study makes the following assumptions:

- Gateway clock synchronization is high to minimize jitter related pseudorange errors
- Negligible multipath propagation effects
- Received signals does not experience any terrain related propagation errors
- There is negligible contributions form sources of radio frequency Interference

These assumptions are essential to producing a working model and may be modified as data becomes available. Investigating other components and including contribution into the TOA variance equation (20) produces an accurate TOA variance model for LoRa.

C. PATHLOSS MODELS FOR LoRa

The signal path loss models are described extensively in work by Erunkulu *et al.* [21]. The Ericsson 9999 model was used in this study and is given by:

$$\begin{aligned} Eric_{9999} = {} & a_0 + a_1 log_{10}(d) + a_2 log_{10}(Tx_{height}) \\ & + a_3 log_{10}(Tx_{height}) + log_{10}(d) \\ & + 0.2(log_{10}(((11.75 \times Rx_{height})^2))) + g_f \end{aligned} \tag{25}$$

where a_0, a_1, a_2, a_3 and g_f are defined as:

$$\begin{aligned} a_0 &= 45.95 \\ a_1 &= 100.6 \\ a_2 &= 12.0 \\ a_3 &= 0.1 \\ g_f &= 44.49 log10(f) - 4.78((log10(f))^2) \end{aligned} \tag{26}$$

Figure 4 shows the received signal strength graph of the Ericsson9999 model. Figures showing the signal strength in our chosen geographical area are in section IV-A.

D. TYPES OF ACCURACY USED IN NAVIGATION

The types of accuracy commonly used in navigation are absolute accuracy and repeatable accuracy. Absolute accuracy is the conformance of a system-generated location to the true measured location, while repeatable represents the conformance of the node's current position to the previously measured position using the same system [3]. This paper focuses on developing the repeatable accuracy model for LoRa and its performance over a chosen geographical area.

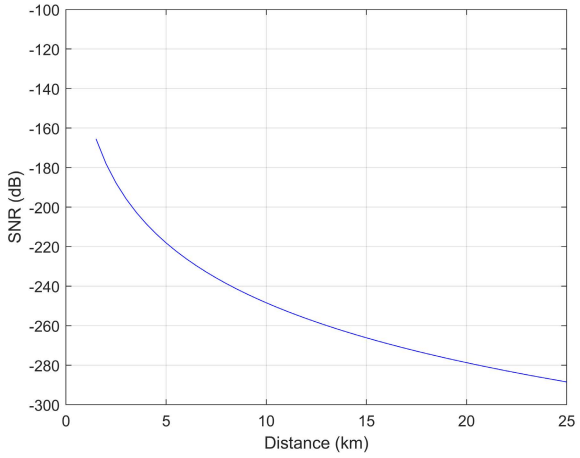

FIGURE 4. Ericsson 9999 SNR graph.

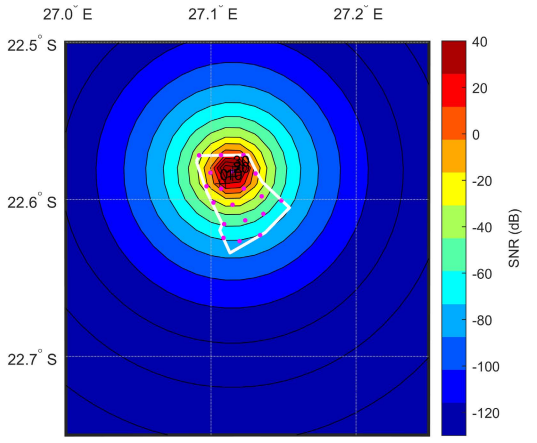

FIGURE 5. Ericsson 9999 Signal Strength: 1500 m gateway separation at SF12.

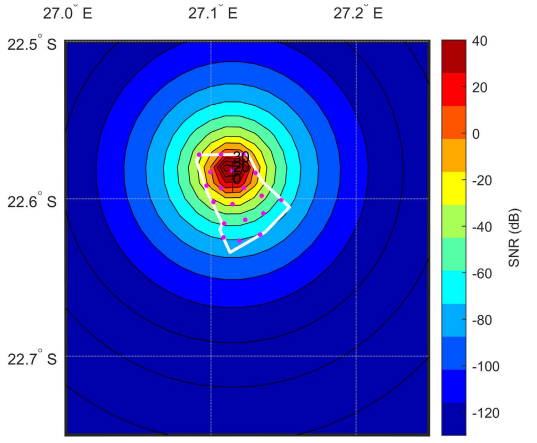

FIGURE 6. Ericsson 9999 Signal Strength: 1500 m gateway separation at SF10.

IV. RESEARCH METHOD

This section describes the position accuracy method proposed for LoRa using the coverage criteria and the gateway deployment strategies to achieve a 20 m accuracy in most parts of the chosen area over which coverage is desired. Currently there is no standard specifying repeatable accuracy for LoRa in mission critical applications. The 20 m accuracy is chosen for comparison against eLoran.

A. DESCRIPTION OF THE POSITION ACCURACY METHOD

Position accuracy is determined by dividing the geographical area into equal grid points. The 95^{th} percentile repeatable accuracy, R_{acc} in meters at each grid point is determined using:

$$R_{acc} = 1.7308\sqrt{\text{tr}(G^T W G^{-1})} \tag{27}$$

where G is given by

$$G = \begin{Bmatrix} sin(\eta_1) & cos(\eta_1) & 1 \\ sin(\eta_2) & cos(\eta_2) & 1 \\ sin(\eta_3) & cos(\eta_3) & 1 \\ sin(\eta_n) & cos(\eta_n) & 1 \end{Bmatrix} \tag{28}$$

and η_n are the gateways (Tx) bearings from the receiver (Rx) nodes.

The covariance matrix is:

$$\sigma^2(\mu) = \begin{Bmatrix} \sigma_{11}^2 & 0 & 0 \\ 0 & \sigma_{22}^2 & 0 \\ 0 & 0 & \sigma_{33}^2 \end{Bmatrix} \tag{29}$$

The inverse of equation 29 is assigned as a weighting in the receiver's position calculation.

B. DEPLOYMENT OF THE GATEWAYS IN THE COVERAGE AREA

First, we propose a gateway arrangement forming equilateral triangles of sides equal to 1000 m, 400 m and 200 m. The authors discussed the principle of arranging equilateral triangles in [22]. Each configuration's accuracy performance was analysed to determine the best configuration that achieves the desired 20 m position accuracy. The 20 m performance figure of merit is chosen here for LoRa to meet the theoretical accuracies proposed for TDOA based navigation by LoRa of 20 m - 200 m [12]. An accomplishment of these stipulated accuracies would make LoRa a valuable candidate in the navigation receiver proposed by Johnson *et al.* [5]. Once the locations of the gateways in a geographical area are known, we divided the geographical area into grid points of equal size. At each grid point, the algorithm determined the SNR from the overall received signal and the system noise, N_{oise} given by:

$$N_{oise} = KTB \tag{30}$$

where K is the Boltzmann constant equal to $1.38 \times 10^{-23} J/K$, T is the temperature in Kelvin, and B is the bandwidth of the system in Hz.

This study assumed that system noise is the dominant noise. The received signal power is equal to the difference between the transmitted power and the power lost along the propagation path estimated using Ericsson 9999 as described by [21]. Ericsson 9999 model can model path loss for frequencies up to 2GHz.

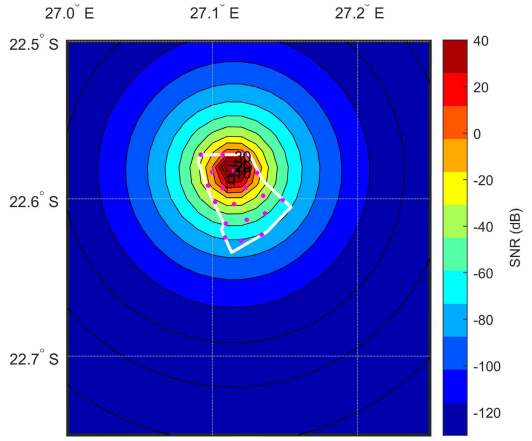

FIGURE 7. Ericsson 9999 Signal Strength: 1500 m gateway separation at SF8.

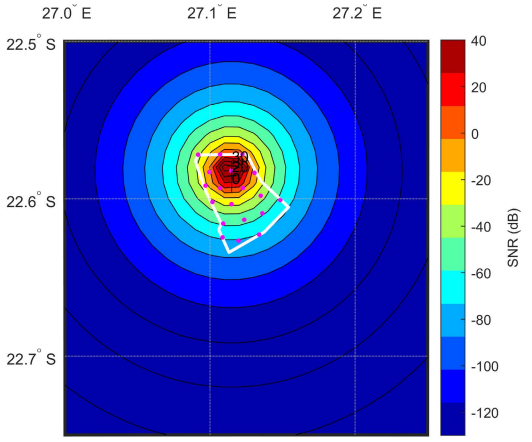

FIGURE 8. Ericsson 9999 Signal Strength: 1500 m gateway separation at SF7.

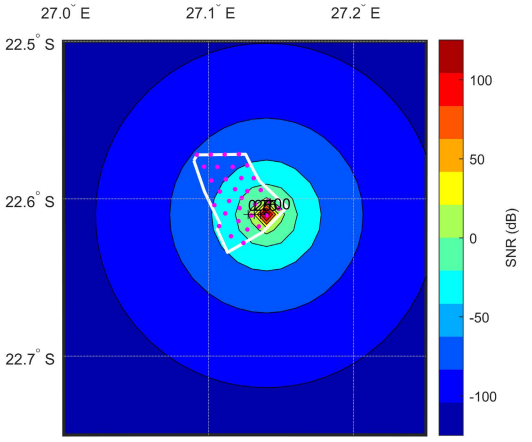

FIGURE 9. Ericsson 9999 Signal Strength: 1000 m gateway separation at SF12.

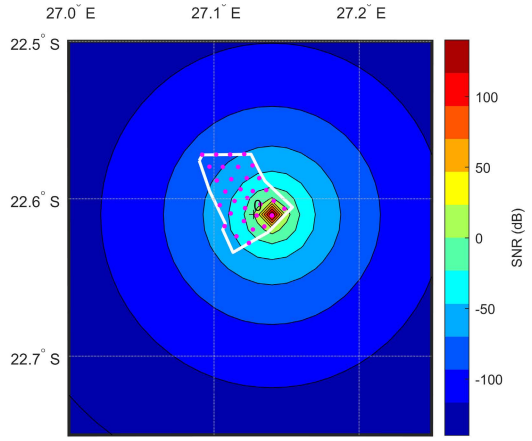

FIGURE 10. Ericsson 9999 Signal Strength: 1000 m gateway separation at SF10.

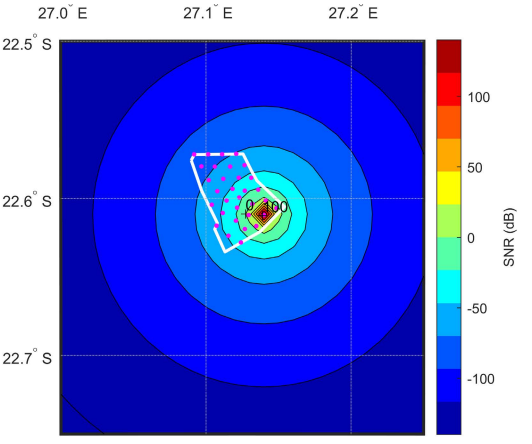

FIGURE 11. Ericsson 9999 Signal Strength: 1000 m gateway separation at SF8.

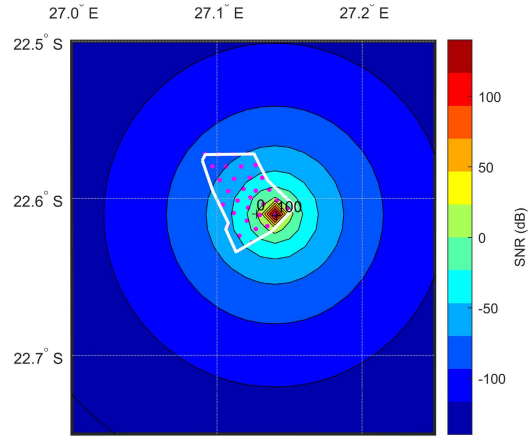

FIGURE 12. Ericsson 9999 Signal Strength: 1000 m gateway separation at SF7.

There is a minimum SNR threshold for any given SF, below which LoRa signals are deemed unusable. In our model, this is considered coverage criteria, and thus any gateway whose SNR is below this threshold would not be used in determining the node's position accuracy. In cases where there are fewer than three gateways, the node's position cannot be determined. Otherwise, the repeatable accuracy is determined. The reciprocity principle is used to determine the node position accuracy, assuming that the gateway is a transmitter and the node is a receiver. This setup would be similar to eLoran.

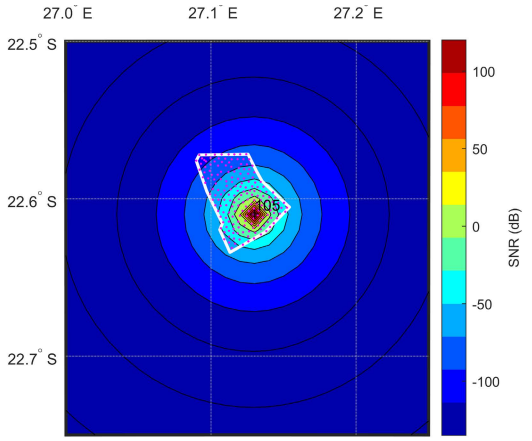

FIGURE 13. Ericsson 9999 Signal Strength: 400 m gateway separation at SF12.

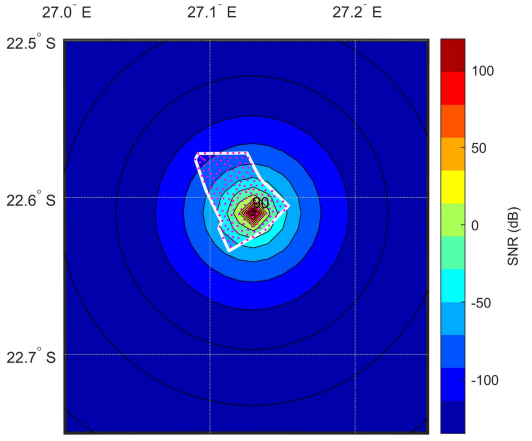

FIGURE 14. Ericsson 9999 Signal Strength: 400 m gateway separation at SF10.

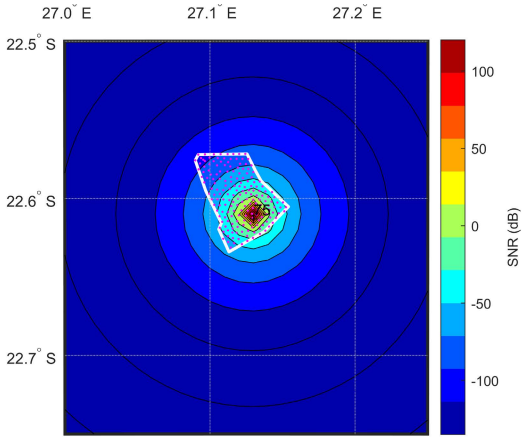

FIGURE 15. Ericsson 9999 Signal Strength: 400 m gateway separation at SF8.

The following section describes the simulation results for different LoRa gateways separation distances and spreading factors configurations.

V. RESULTS AND DISCUSSION

The signal strength of sample gateways for the 400 m, 1000 m and 1500 m gateway separation distances at different SFs' are illustrated in figures 5 to 16. The magenta dots represent gateways in all illustrations, while the white borderline is the coverage area boundary. The results in figures 5 to 16 suggest that for any given SF, increased gateway distance leads to an improved SNR across the coverage area. The results also suggest no significant change in SNR across the coverage area when SF is varied while keeping the same gateway separation distance. The plots figures 17, 18 19, 20, 21, 23, 24 and 25 calculated using equation 27 show simulated repeatable accuracy results in the coverage area demarcated by the white line. The bar graph in fig. 26 displays the values of repeatable accuracy for a specific gateway separation and spreading factor.

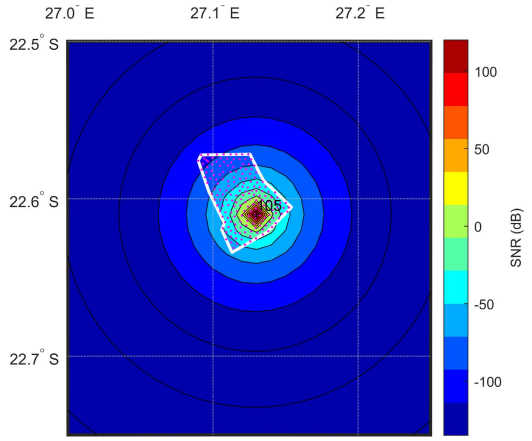

FIGURE 16. Ericsson 9999 Signal Strength: 400 m gateway separation at SF7.

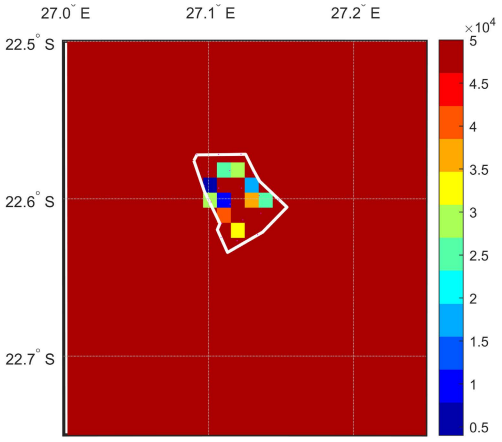

FIGURE 17. Ericsson 9999 Signal Strength: 1500 m gateway separation at SF8 BW 125kHz.

A. COVERAGE AREA REPEATABLE ACCURACY

B. REPEATABLE ACCURACY

The following section provides an analysis of our experimental results. The results suggest that an increased SF at the same gateway separation distance improves the repeatable accuracy significantly as seen by comparing figure 24 and 25. Figure 26 illustrate the changes in repeatable accuracy when increasing the spreading factor for gateways spaced 400 m,

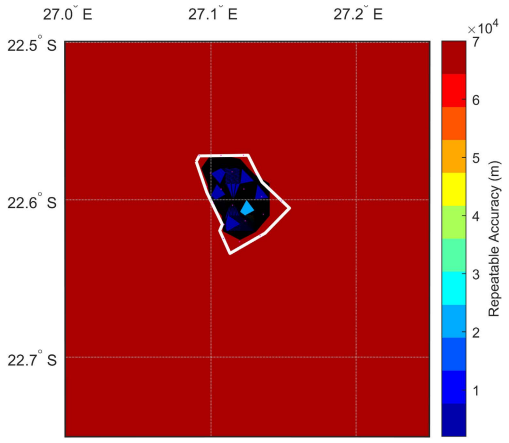

FIGURE 18. Ericsson 9999 Signal Strength: 1500 m gateway separation at SF10 BW 125kHz.

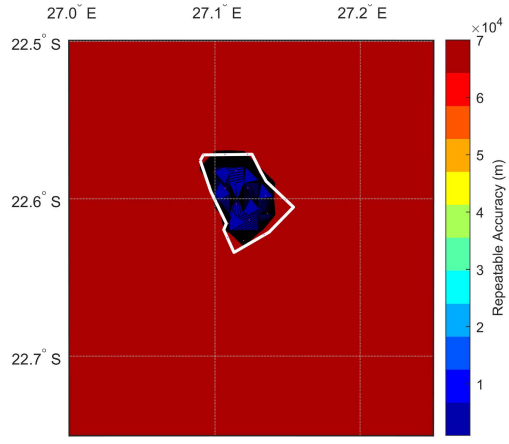

FIGURE 19. Ericsson 9999 Signal Strength: 1500 m gateway separation at SF12 BW 125kHz.

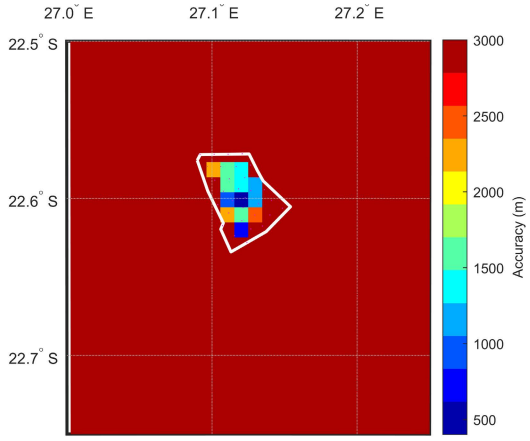

FIGURE 20. Ericsson 9999 repeatable accuracy: 1000 m gateway separation at SF12 BW 125kHz.

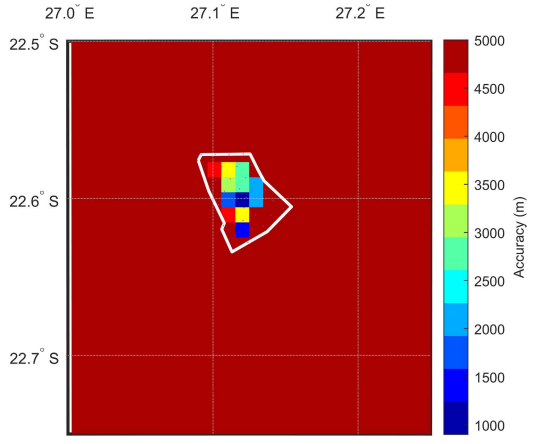

FIGURE 21. Ericsson 9999 repeatable accuracy: 1000 m gateway separation at SF12 BW 125kHz.

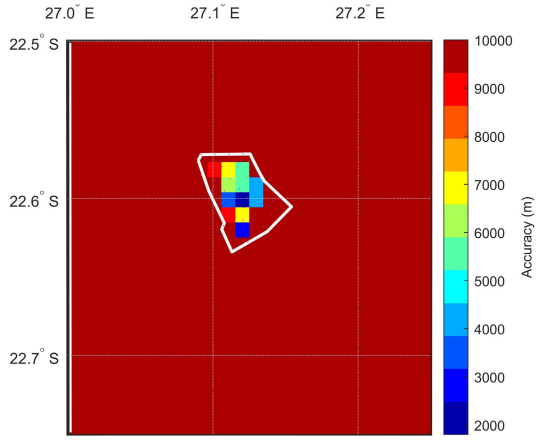

FIGURE 22. Ericsson 9999 repeatable accuracy: 1000 m gateway separation at SF12 BW 125kHz.

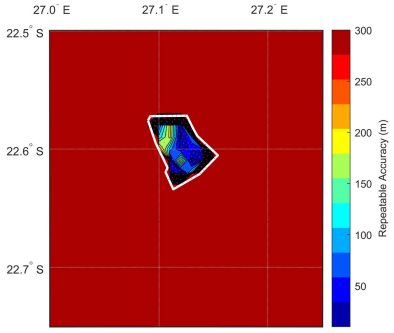

FIGURE 23. Ericsson 9999 repeatable accuracy: 400 m gateway separation at SF8 BW 125kHz.

1000 m and 1500 m, respectively. In each configuration, we assumed that the receiver moves across the grid created using the procedure outlined in section IV-A. The resolution of the grid is 0.01° in the latitude and longitudes. The TOA variance using equation (15) is determined using each gateway SNR. In these simulations, the BW of the system was kept constant, and the same path loss model was used to determine the signal strengths at different distances from the gateways using equation 25.

At an SF of 8, in the 1500 m separation, the best repeatable accuracy was over 2000 m. This result is high and unacceptable compared to the 20 m standard. Increasing the spreading factor to 10 and 12 led to an accuracy of 1443 m and 1249 m, respectively. This value of repeatable accuracy still fell short

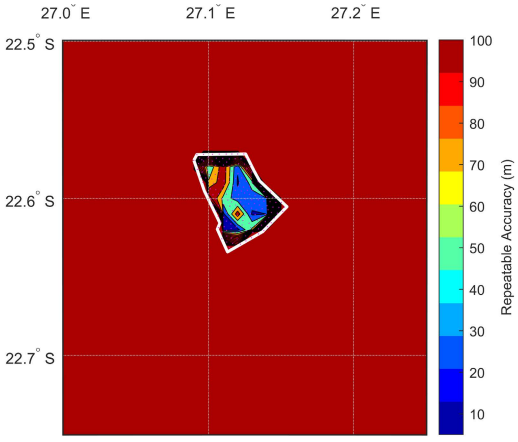

FIGURE 24. Ericsson 9999 repeatable accuracy: 400 m gateway separation at SF10 BW 125kHz.

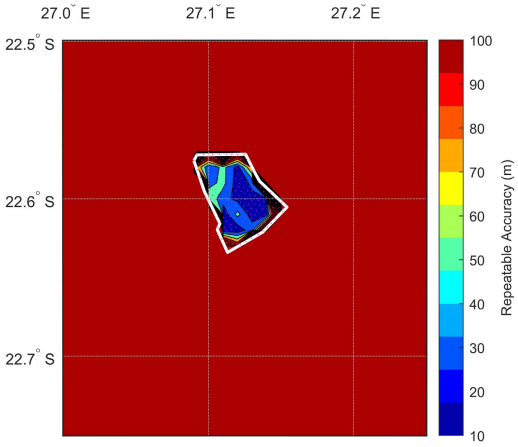

FIGURE 25. Ericsson 9999 repeatable accuracy: 400 m gateway separation at SF 12 and BW 125kHz.

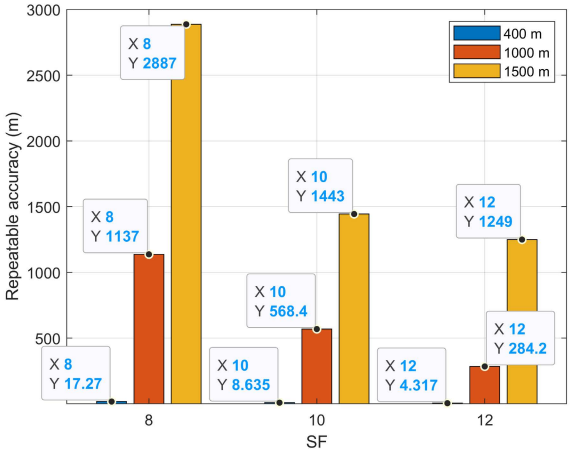

FIGURE 26. Ericsson 9999 repeatable accuracy: 400 m, 1000 m, and 1500 m gateway separation at SF 8,10,12 and BW 125kHz.

of the desired 20 m target. A contour plot of the repeatable accuracy of the coverage area is illustrated in figure 17, 18 and 19 for SF 8,10 and 12.

For the 1000 m separation, we observed that an SF of 8 results in repeatable accuracy of 1137 m. Increasing the SF to 10 and 12 results in an accuracy of 568.4 m and 284.2 m, respectively. The result is better than the one for 1500m separation distance, but it is still below the target threshold. The contour plots in Figures 20, 21 and 22 illustrate the repeatable accuracy for SF 8,10 and 12 respectively.

Finally, for the 400 m separation distance, the observed repeatable accuracies for SF8, 10 and 12 are 17.27 m, 8.635 m and 4.314 m, respectively. These values are comparable to those obtained using the most popular navigation systems.

VI. CONCLUSION

Our simulated repeatable accuracy results compare well with the range observed by other researchers investigating LoRa for navigation applications listed in table 1. Most of the authors cite in this table were not explicit about the gateway separation distances, and in some cases, the gateways used were of a public network.

While we were able to show that our results are consistent with the work of other researchers, there are some limitations in our model. Specifically, the obtained repeatable accuracy values may be worse than projected due to the following:

- our model did not incorporate stochastic channel interference some researchers have observed in 900MHz by authors such as [23] and [24],
- our model did not incorporate the effects of meteorological parameters on a LoRa signal.

Since LoRa nodes and gateways cost a fraction of a typical navigation system, decreasing gateway spacing may improve accuracy. The results of this work demonstrate that LoRa has the potential to become a signal of opportunity for navigation purposes similar to the work of [5].

REFERENCES

[1] Deere and Company. (Nov. 2020). *Precision AG Technology*. John Deere. [Online]. Available: https://www.deere.com/en/technology-products/precision-ag-technology/

[2] DJI. (Nov. 2020). *Technology Inspires Growth*. Dji. [Online]. Available: https://ag.dji.com/?site=brandsite&from=homepage

[3] J. Safar, "Analysis, modelling and mitigation of cross-rate interference in enhanced loran," Ph.D. thesis, Dept. Radio Eng., Czech Tech. Univ., Prague, Czech Republic, 2014.

[4] C. J. Hegarty, *Understanding GPS/GNSS: Principles and Applications*, 3rd ed, London, U.K.: Artech House, 2017, p. 1064.

[5] G. Johnson and P. Swaszek. *Feasibility Study of R-Mode Combining MF DGNSS, AIS, and eLoran Transmissions*. Accessed: Jun. 1, 2021. [Online]. Available: https://www.iala-aism.org/content/uploads/2016/08/accseas_r_mode_feasibility_study_combined_dgnss_ais_and_eloran.pdf

[6] M. Kayton and W. Fried, *Avionics Navigation Systems*, 2nd ed. New York, NY, USA: Wiley, 1997.

[7] I. Baumann. (Sep. 2017). *Imo and the GNSS*. [Online]. Available: https://insidegnss.com/imo-and-the-gnss/

[8] M. C. Bor, J. Vidler, and U. Roedig, "LoRa for the Internet of Things," in *Proc. Int. Conf. Embedded Wireless Syst. Netw.*, 2016, pp. 361–366. [Online]. Available: http://eprints.lancs.ac.U.K./77615/

[9] T. R. Haritsa, B. M. Yashu, U. V. Kumar, and M. N. Suma, "Mathematical characterization and simulation of Lora," *Wireless Pers. Commun.*, vol. 115, no. 2, pp. 1481–1506, Nov. 2020, doi: 10.1007/s11277-020-07638-y.

[10] N. Podevijn, D. Plets, J. Trogh, L. Martens, P. Suanet, K. Hendrikse, and W. Joseph, "TDoA-based outdoor positioning with tracking algorithm in a public Lora network," *Wireless Commun. Mobile Comput.*, vol. 2018, pp. 1–9, May 2018.

[11] C. Gu, L. Jiang, and R. Tan, "LoRa-based localization: Opportunities and challenges," 2018, *arXiv:1812.11481*.
[12] (Jan. 15, 2018). LoRa Alliance Strategy Committee. *LoRaWAN Geolocation Whitepaper*. [Online]. Available: https://docs.wixstatic.com/ugd/
[13] B. C. Fargas and M. N. Petersen, "GPS-free geolocation using LoRa in low-power WANs," in *Proc. Global Internet Things Summit (GIoTS)*, 2017, pp. 1–6, doi: 10.1109/GIOTS.2017.8016251.
[14] B. Alan, *Wireless Positioning Technologies and Applications*, 2nd ed. Norwood, MA, USA: Artech House, 2016.
[15] N. Blenn and F. Kuipers, "LoRaWAN in the wild: Measurements from the things network," 2017, *arXiv:1706.03086*.
[16] *M. S. Thesis Investigation on Time-of-Arrival Estimation for the LoRa Network*, Delft Univ. Technology, Delft, The Netherlands, 2019.
[17] R. Lie. (2018). *LoRa/LoRaWAN tutorial 17: LoRa Packet Format, Time on Air and Adaptive Data Rate*. [Online]. Available: https://www.mobilefish.com/developer/lorawan/
[18] Semtech Corporation. (2015). *LoRa Modulation Basics*. Semtech Corporation, Camarillo, CA, USA. Accessed: Apr. 19, 2020. [Online]. Available: https://www.semtech.com/uploads/documents/an1200.22.pdf
[19] C. K. Lebekwe, A. Yahya, and I. Astin, "An improved accuracy model employing an e-Navigation system," in *Proc. 9th IEEE Annu. Ubiquitous Comput., Electron. Mobile Commun. Conf. (UEMCON)*, Nov. 2018, pp. 152–158.
[20] F. M. B. A. El-Aziz, E. El-Deen F. Abd-El kawy, A. Khamis, and D. Zydek, "Integrity performance of Egyptian eLoran system for maritime application," in *Proc. 26th Int. Conf. Syst. Eng. (ICSEng)*, Dec. 2018, pp. 1–6.
[21] O. O. Erunkulu, A. M. Zungeru, C. K. Lebekwe, and J. M. Chuma, "Cellular communications coverage prediction techniques: A survey and comparison," *IEEE Access*, vol. 8, pp. 113052–113077, 2020.
[22] L. Kolobe, C. K. Lebekwe, and B. Sigweni, "LoRa network planning and deployment: A terrestrial navigation application," *IEEE Access*, vol. 9, pp. 126670–126683, 2021.
[23] K. Staniec and M. Kowal, "LoRa performance under variable interference and heavy-multipath conditions," *Wireless Commun. Mobile Comput.*, vol. 2018, pp. 1–9, Apr. 2018.
[24] L. Beltramelli, A. Mahmood, M. Gidlund, P. Osterberg, and U. Jennehag, "Interference modelling in a multi-cell Lora system," in *Proc. 14th Int. Conf. Wireless Mobile Comput., Netw. Commun. (WiMob)*, Oct. 2018, pp. 1–8.

CASPAR K. LEBEKWE (Member, IEEE) received the M.Eng. degree in electronics and communications engineering from the University of Bath, in 2008, and the Ph.D. degree in electrical and electronics engineering, sponsored by the General Lighthouse Authorities from the University of Bath. His Ph.D. project was focused on eLoran Service Volume Coverage Prediction. He is currently a Senior Lecturer with the Botswana International University of Science and Technology, where he teaches optical communications, antennas and propagation, discrete mathematics, telemetry, remote control, and electromagnetic field theory.

LONE KOLOBE received the B.Eng. and M.Eng. degrees in computer and telecommunications engineering from the Electrical, Computer and Telecommunications Department, Botswana International University of Science and Technology (BIUST), Palapye, Botswana, in 2017 and 2021, respectively.

BOYCE SIGWENI (Member, IEEE) received the B.Sc. degree in computer engineering from the University of KwaZulu-Natal, in 2007, the M.Sc. degree from North-West University, in 2011, and the Ph.D. degree in empirical software engineering from Brunel University London, U.K. He is currently a Senior Lecturer in computer engineering with the College of Engineering, Botswana International University of Science and Technology (BIUST). Prior to joining BIUST, he was a Computer Science Lecturer with North-West University. His research interests include powerline communication, next generation networks, and empirical software engineering.

ADAMU MURTALA ZUNGERU (Senior Member, IEEE) received the B.Eng. degree from the Federal University of Technology, Minna, Nigeria, the M.Sc. degree from Ahmadu Bello University, Zaria, Nigeria, and the Ph.D. degree from Nottingham University, U.K. He was a Research Fellow with the Massachusetts Institute of Technology (MIT), USA, where he also obtained a Postgraduate Teaching Certificate, in 2014. He is currently working as a Professor and the Head of the Department of Electrical, Computer, and Telecommunications Engineering, Botswana International University of Science and Technology (BIUST). Before joining BIUST, in 2015, he was a Senior Lecturer and the Head of the Electrical and Electronics Engineering Department, Federal University Oye-Ekiti, Nigeria. He is a Registered Engineer with the Council for The Regulation of Engineering in Nigeria (COREN) and the Association for Computing Machinery (ACM), USA. He is an Inventor of a Termite-hill routing algorithm for wireless sensor networks. He has two of his patent applications registered with the World Intellectual Property Organization (WIPO). He has also authored five academic books and over 60 international research articles in reputable journals, including the IEEE Systems Journal, the IEEE Internet of Things Journal, IEEE Access, *JNCA* (Elsevier), and others, with over 900 citations and H-index of 14. He is currently serving as an Associate Editor for IEEE Access. He has also served as an International Reviewer for the IEEE Transactions on Industrial Informatics, the IEEE Sensors, IEEE Access, the IEEE Transactions on Mobile Computing, the IEEE Transactions on Sustainable Computing, *JNCA* (Elsevier), and numerous others. He has also served as the Chairperson of the IEEE Botswana Sub-Section (2019–2020), and as the IEEE Region 8 Vitality and Development Subcommittee Member.